ARTICLES
PUBLISHED ONLINE: 10 FEBRUARY 2013 | DOI: 10.1038/NCLIMATE1817
nature climate change

Atmospheric verification of anthropogenic CO_2 emission trends

Roger J. Francey[1]*, Cathy M. Trudinger[1]*, Marcel van der Schoot[1], Rachel M. Law[1], Paul B. Krummel[1], Ray L. Langenfelds[1], L. Paul Steele[1], Colin E. Allison[1], Ann R. Stavert[1], Robert J. Andres[2] and Christian Rödenbeck[3]

International efforts to limit global warming and ocean acidification aim to slow the growth of atmospheric CO_2, guided primarily by national and industry estimates of production and consumption of fossil fuels. Atmospheric verification of emissions is vital but present global inversion methods are inadequate for this purpose. We demonstrate a clear response in atmospheric CO_2 coinciding with a sharp 2010 increase in Asian emissions but show persisting slowing mean CO_2 growth from 2002/03. Growth and inter-hemispheric concentration difference during the onset and recovery of the Global Financial Crisis support a previous speculation that the reported 2000–2008 emissions surge is an artefact, most simply explained by a cumulative underestimation (~9 Pg C) of 1994–2007 emissions; in this case, post-2000 emissions would track mid-range of Intergovernmental Panel on Climate Change emission scenarios. An alternative explanation requires changes in the northern terrestrial land sink that offset anthropogenic emission changes. We suggest atmospheric methods to help resolve this ambiguity.

On century and multi-decade time frames, increasing growth of CO_2 in the global atmosphere is attributed[1,2] to anthropogenic emissions comprising fossil-fuel combustion and cement manufacture[3] (FF) and land-use change[4] (LUC). On sub-decadal time frames, critical for early verification of post-Kyoto emissions and mitigation measures, detection of changes in CO_2 growth (dC/dt) in response to changed trends in FF+LUC is masked by natural 3–5 year interannual variability (IAV). Co-variation in CO_2 and its stable carbon isotopic ratio ($^{13}C/^{12}C$) shows the IAV influence is primarily through CO_2 exchange involving carbon that has experienced terrestrial photosynthesis[2] (Supplementary Figs S1 and S2), which is forced in turn by climate variability associated with the influence of El Niño/Southern Oscillation (ENSO) and explosive volcanoes; exchange with oceans involves carbon isotopically equilibrated with inorganic sources and with little impact on atmospheric $^{13}C/^{12}C$ values.

A previous study[5] of trends in the global carbon budget data to 2007/08 revealed inconsistencies between smoothed 2000–2008 dC/dt and reported global anthropogenic emissions and speculated on the cause being an underestimate of emissions around 2000. Here, we re-examine that result informed by the atmospheric response at the time of the onset[6] and recovery[7] from the Global Financial Crisis (GFC); we also use revised LUC (ref. 8), decreased uncertainty[9] in the synthesis of industry estimates of global emissions, but increased uncertainty in Chinese emissions[10,11]. Apparent global carbon budget anomalies[12] are amplified by recent reported slowing of terrestrial[13] and oceanic[14,15] uptake of CO_2.

Our analysis now includes atmospheric transport modelling, stable carbon isotope data, and CO_2 data from other networks. Although our method for determining dC/dt and its uncertainty is the same as previously described[5] (Methods), we have refined our accounting of IAV using independent data on wildfires[16] and a modelled temporal response to volcanic explosions[17].

As anthropogenic emissions are predominantly located in the Northern Hemisphere, we pay particular attention to the inter-hemispheric CO_2 difference, ΔC_{n-s}. This difference is less sensitive to IAV than dC/dt, because IAV is mostly generated in the tropics[18], mixes into both hemispheres and is largely cancelled in determining ΔC_{n-s}. Hence, changes in Northern Hemisphere emissions may be detected more promptly in ΔC_{n-s} than in smoothed dC/dt.

Anthropogenic emission rates

Our primary focus is the dynamic atmospheric response to unprecedented changes in reported FF emissions, those associated with a 29% increase in 2000–2008[6] and the 5.9% annual jump in 2010[7]. During the 2000–2008 surge[6], FF adds an extra ~0.3 Pg C yr^{-1}; in 2010, the annual increase is 0.51 Pg C (ref. 7).

The reported anthropogenic emission-rate changes on decadal time frames (long compared with inter-hemispheric mixing and aiding suppression of IAV in the atmospheric data by averaging over 2–3 ENSO cycles) are shown in Fig. 1. We select decades that emphasize emission-rate changes. Changes in FF dominate as indicated by including FF+LUC changes. The 1990s (low) and 2000s (high) decadal increases are unmatched. As these emissions are predominantly from mid northern latitudes (Northern Hemisphere) and exceed typical co-located natural annual net exchanges of terrestrial or ocean sinks, they are a primary influence on both dC/dt and ΔC_{n-s}.

Atmospheric data

Figure 2a shows our most precise indication of the recent slowing trend in global CO_2 growth using stringently selected baseline data measured at Cape Grim (CGO, 41° S, 141° E) from 2002

[1]Centre for Australian Weather and Climate Research, CSIRO Marine and Atmospheric Research, Aspendale, Victoria 3195, Australia, [2]Carbon Dioxide Information Analysis Center, Oak Ridge National Laboratory, Oak Ridge, Tennessee 37831-6290, USA, [3]Max-Planck-Institute for Biogeochemistry, Hans-Knoell-Straße 10, 07745 Jena, Germany. *e-mail: roger.francey@csiro.au; cathy.trudinger@csiro.au.

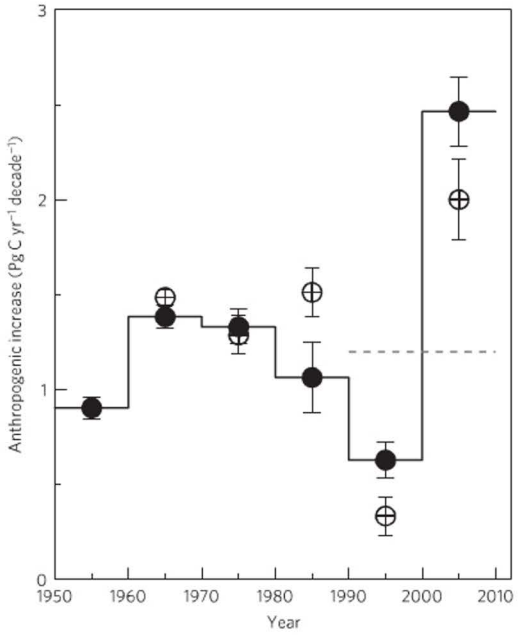

Figure 1 | Decadal rates of increase in anthropogenic emissions since 1950. Filled circles connected by a step plot show the slope of linear regressions through each decade of annual (FF) fluxes from 1950 to 2009[3]. Open crossed circles show similar values when LUC estimates from 1960 are added[8]. Error bars are ± the standard error in regression slope. The dashed grey line shows alternative FF growth used below in model sensitivity studies. The figure is not significantly different using BP (British Petroleum[34]) or EDGAR (Emissions Database for Global Atmospheric Research[35]) emission compilations.

with the ultraprecise continuous LoFlo system[19]. The selection represents air from a large proportion of the Southern Hemisphere troposphere (>100° longitude, ~50° latitude and 8 km altitude)[5] with no recent exposure to land.

Figure 2b shows 5-year smoothed dC/dt and demonstrates excellent agreement between LoFlo data and intermittent CGO data from the independently operated CSIRO (Commonwealth Scientific and Industrial Research Organisation) Global Atmospheric Sampling network[20] (Methods). These flask measurements extend back to 1992 (ref. 5) using consistent baseline sampling criteria and are the main source of data used in this article. (Sampling and measurement consistency is supported by the remarkable uniformity in baseline selected monthly CO_2 and $\delta^{13}CO_2$ from widely spread flask mid-to-high latitude Southern Hemisphere sampling sites; Supplementary Fig. S1.)

Included in Fig. 2b are 5-year smoothed dC/dt from Mauna Loa (MLO, 20° N, 156° W) and Alert (ALT, 82° N, 63° W). All three sites have similar mean trends, and Northern Hemisphere records remain statistically similar to CGO throughout, but with larger uncertainty (indicating reduced spatial representativeness); the apparent departure between Northern Hemisphere and Southern Hemisphere trends after ~2009 may have a contribution from possible end-effects in the 5-year spline (much more pronounced with the large Northern Hemisphere seasonality) but may also be associated with emission changes discussed in the next paragraph. The dC/dt increase during the 1990s and slowing in the 2000s is opposite to the decadal trends in emissions shown in Fig. 1. Significantly, the mean dC/dt remains below the respective hemisphere 5-decade trends—at MLO and South Pole (SPO, 90° S)—through to 2011, contrary to perceptions of accelerating emissions growth and slowing natural sinks over recent decades.

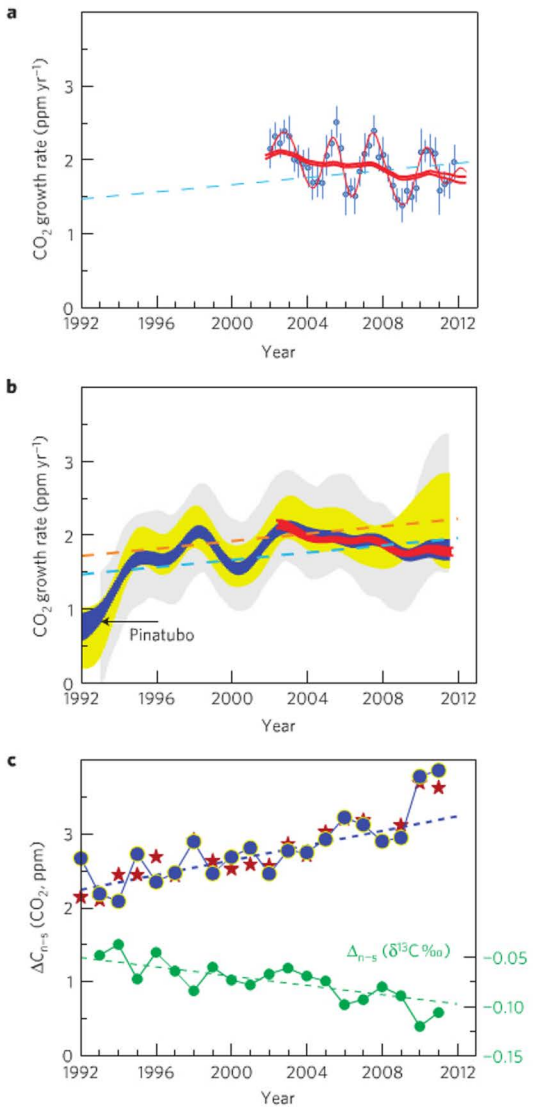

Figure 2 | Measurements of atmospheric CO_2. a, Slowing CO_2 growth (dC/dt) using precise continuous LoFlo monitoring[19] at (CGO): blue points are annual differences in monthly mean CO_2 concentration ($\pm 1\sigma$ uncertainties), using hours selected to maximize spatial representativeness. The smoothed 1.8-yr (ref. 36; thin red) and 5-yr (ref. 37; $\pm 1\sigma$, thick red) curves are derived from the monthly values. The light-blue dashed line is an extrapolated linear regression fitted to 50 yr^2 of SPO dC/dt. **b**, Uncertainty bands[37] of 5-yr smoothed (dC/dt) using CSIRO flasks collected from clean-air sectors at CGO (blue), MLO (yellow) and ALT (grey); $\pm 3\sigma$ uncertainties in monthly mean concentrations are propagated. The red curve is from **a**. Dashed lines are the extrapolated 5-decade linear regressions through MLO (orange) and SPO (blue) dC/dt. **c**, Inter-hemispheric differences (MLO-CGO) using annual average concentrations for CO_2 (blue) and $\delta^{13}CO_2$ (green). Thin dashed lines are linear regressions through 1992–2009 values. Brown stars are NOAA CO_2 data[38].

The MLO–CGO annual mean difference, $\Delta C_{MLO-CGO}$, is shown in Fig. 2c. The 2010 and 2011 values are more than three times the y standard error in a linear regression through the 1992–2009 differences. We interpret this as the first clear evidence for an atmospheric response to anthropogenic emission changes on annual time frames. The synchronous $\delta^{13}CO_2$ drop, although noisier, is

consistent with a Northern Hemisphere anthropogenic or terrestrial (rather than ocean) CO_2 increase (Supplementary Fig. S2). An examination of National Oceanic and Atmospheric Administration (NOAA, USA) data suggests that the effect is detected earlier and with better signal/noise at Pacific monitoring sites (Supplementary Figs S3 and S4). Interpretation on such a brief time frame requires consideration of the time to achieve equilibration between hemispheres, but first we compare global emission and atmospheric trends over periods that are long compared with inter-hemispheric mixing (relying on atmospheric mixing for global integration).

Atmospheric versus emission trends

Figure 3 compares reported FF+LUC trends over the past two decades with dC/dt trends modified to account for possible natural contributions to atmospheric changes (IAV; Methods, Supplementary Figs S5 and S6). Comparing Fig. 3 with Fig. 2b, the dC/dt slowing since 2002/3 is marginally offset (flattened) when known natural variability is taken into account; enhanced La Niña conditions, volcanic activity and reduced wildfire emissions after 2008 all contribute reduced CO_2 growth. This natural variability complicates unambiguous identification of a GFC influence in 2008/9 from the CO_2 growth rate.

FF+LUC and dC/dt-IAV are overlaid in 2004–2007 by a relative shift in the axes of 5.3 Pg C yr^{-1} (accounted for by other carbon budget components). The 2004–2007 period was selected for alignment because volcanic activity is low, there is no obvious anomalous ENSO behaviour, it immediately precedes the GFC, atmospheric dC/dt is globally consistent and, for many regions, methodologies for determining national emissions have matured compared with earlier times. As we have suppressed known interannual influences on dC/dt, longer-term changes in emissions and those in dC/dt–IAV should be comparable.

The 1993 (post-Pinatubo)-to-2004 area between FF+LUC and dC/dt–IAV amounts to a cumulative 8.8 Pg C budget anomaly over the period. An underestimation of FF+LUC, and/or increase in natural sinks of this magnitude and temporal evolution, is required to reconcile emissions with CO_2 changes. Note that biofuel burning[21], of similar size to LUC, may contribute to this anomaly (if not already included in fire and LUC estimates). Here we consider that LUC and biofuel burning at northern latitudes are unlikely to provide sufficiently large temporal changes to explain the global budget anomaly and inter-hemispheric gradient constraints (compared with larger terrestrial and FF fluxes that are more sensitive to climate and socioeconomic forcing respectively). This anomaly remains a major challenge to global atmospheric verification over the past two decades.

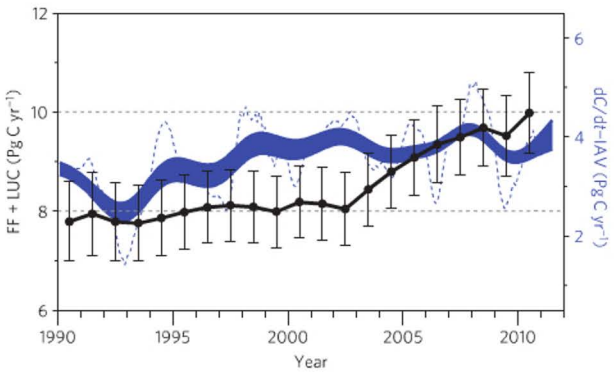

Figure 3 | Comparison of anthropogenic emissions and atmospheric trends. Annual anthropogenic emission (FF+LUC, black) estimates are plotted on the left axis[3,8] with horizontal grid lines. (Note: the FF uncertainty[9] is small compared with that in LUC.) On the right axis, also spanning 6 Pg C yr^{-1}, the blue band bounds the $\pm 3\langle\sigma\rangle$ uncertainty in dC/dt–IAV, using the CGO record with 5-yr smoothing, adjusted for wildfires, volcanoes and ENSO; the light blue dotted curve is dC/dt–IAV with 1.8-yr smoothing. The right axis is aligned to get overlap of dC/dt–IAV and emissions between 2004 and 2007.

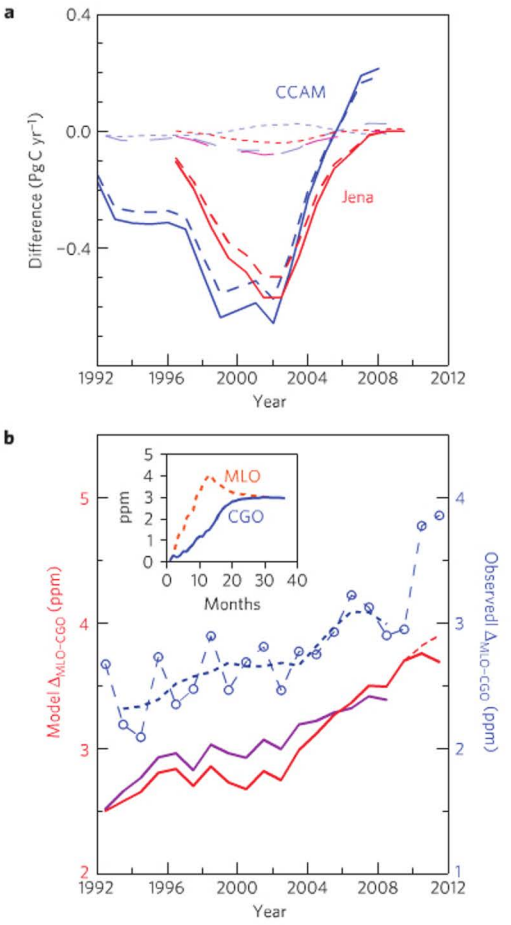

Figure 4 | Transport model diagnostic tests. a, Solid lines show differences between reported and linearly interpolated FF emissions specified for CCAM (ref. 18; blue) and Jena[23] (red) inversion runs (Methods). Respectively, broken lines represent model responses in global sink regions (medium dashes, predominantly land biosphere in North America, Europe, Asia, 20°–90° N); thin long dashes show flux differences for tropical lands, and thin short dashes are for all other regions (mainly ocean). **b**, The inset shows the lagged CGO response to a single, annual, distributed (mainly Northern Hemisphere) emissions pulse, of 6.1 Pg C yr^{-1}, using the CCAM model. Modelled annual inter-hemispheric differences ($\Delta C_{MLO-CGO}$, left axis) are for linearly interpolated (1990–2008) FF emissions[5] (purple) and reported emissions (red); the dashed line is when 2010/11 emission increases are all released from the Asian region. Measured $\Delta C_{MLO-CGO}$ from Fig. 2c (right axis) are shown in blue, offset from model values for clarity; the dashed blue line is a 3-yr running mean through the annual values.

The comparison of anthropogenic emission and global sink trends is often discussed (on time frames long enough to average out IAV) in terms of an air-borne fraction[22] (AF). With these data, two-decade AF = (dC/dt − IAV)/(FF + LUC) is 0.42; combining uncertainties, there is no significant difference between decades: 0.42 ± 0.03 to 0.43 ± 0.03.

CO_2 transport modelling

Atmospheric inversions estimate carbon fluxes by optimally fitting atmospheric CO_2 measurements, usually assuming known FF emissions. We tested the sensitivity to changing the assumed FF emissions (from reported to linearly increasing) using two different inversions[18,23] (Methods). Figure 4a shows the difference in the imposed FF emissions and the inversion's response, which is a change in 20° N–90° N land fluxes almost equalling the change in emissions. The land flux change is small compared with the land flux IAV, suggesting either result is equally plausible (the absolute 20° N–90° N terrestrial values for these model runs are shown in Supplementary Fig. S7). Both cases also fit the atmospheric data (dC/dt and ΔC_{n-s}) equally well (root mean square difference (RMSD) = 1.10 and 1.11 ppm for CCAM (CSIRO Conformal-cubic Atmosphere Model) reported and linear, 1.25 and 1.25 ppm for Jena). Clearly, present global CO_2 inversion implementations are inadequate to distinguish between FF and co-located terrestrial emissions.

Forward runs using the CCAM model are shown in Fig. 4b. The inset shows the evolution of annual CO_2 concentrations at MLO and CGO in response to a FF pulse (mainly in the Northern Hemisphere); the 1–2 year delay in CGO response relative to that at MLO enhances the potential for detection of sudden changes to FF emissions using annual $\Delta C_{MLO-CGO}$.

The fossil contribution to ΔC_{n-s} was assessed using forward runs of the CCAM model with annually varying transport through nudging by NCEP (National Centers for Environmental Protection) winds[24]. $\Delta C_{MLO-CGO}$ differs by up to 0.25 ppm, pivoted around 2000, depending on whether reported or linearly increasing emissions are used (red and purple lines in Fig. 4b). This is smaller than the year-to-year scatter in observed $\Delta C_{MLO-CGO}$ (symbols in Fig. 4b) for reasons likely to involve variations in terrestrial fluxes and inter-hemispheric exchange[25]. However, the correlation between the year-to-year variations in observed and modelled $\Delta C_{MLO-CGO}$ ($r \sim 0.5$) implies that detectability of the alternative fossil scenarios may be improved with a more comprehensive analysis. Meanwhile, consistent with the previous study[5], the blue-dashed three-year running mean through the measured values effectively suppresses year-to-year scatter and shows 2000–2008 values increasing by 0.4 ppm, very similar to the model result with linearly interpolated modelled emissions (0.5 ppm) and half that with the reported emissions (0.8 ppm).

The 2009–2010 increase in $\Delta C_{MLO-CGO}$ far exceeds the modelled response. The gap is only marginally narrowed if modelled emissions are all released in the Asian region. We see no suggestion of a similar increase in $\Delta C_{MLO-CGO}$ around the onset of the 2000–2008 reported emissions surge.

Discussion and conclusions

In terms of global warming and ocean acidification, the most directly relevant result is the persistent slowing from 2002/03 in mean atmospheric CO_2 growth observed in the largest well-mixed volume of the global troposphere.

If this slowing growth is the result of a Southern Hemisphere influence, it is in the wrong direction to support a slowing Southern Ocean sink[26]. If accepted as a sensitive measure of global decadal trends, it is incompatible with recent reports of slowing global terrestrial[13] and oceanic[14,15] sinks (compared with historic trends[1]); for example CO_2 inversions suggest increasing terrestrial sinks from 2003 (Supplementary Fig. S7).

A clear atmospheric response in MLO–CGO annual differences coincides with record 2010 CO_2 emissions from the Asian region[7], the signal being enhanced by slow atmospheric equilibration and possibly by MLO proximity to Asian emission regions. Annual variability in MLO–CGO concentration is clearly influenced by year-to-year changes in inter-hemispheric transport, well described by NCEP reanalysis[24] winds. The failure to detect previous rapid changes in anthropogenic emissions associated with the 2000–2008 emission surge[5] further questions that surge.

Global carbon cycle inversions generally use prescribed fossil emissions with little or no uncertainty. Although political and economic attitudes towards CO_2 emissions have changed over the decades of interest, there has not been a wholesale revision of past data to reflect these changing attitudes. Thus, the reported CDIAC (Carbon Dioxide Information Analysis Center) emission estimates[3] are generally assumed to reflect emission realities within the uncertainties expressed. This assumption is difficult to reconcile with the data presented in Figs 3 and 4. Figure 3 implies that emissions in 2000 are around 1 Pg C higher than the values used to anchor Intergovernmental Panel on Climate Change Special Report on Emissions Scenarios[27]. Anchored on the higher value, post-2000 emissions track mid-to-low range socioeconomic scenarios.

The key message from this work is that atmospheric measurements contain important information about the global carbon budget that is not utilized by present approaches. For example, careful and coordinated selection of data to provide growth rates and annual averages from several established CO_2 monitoring programmes in Asia[28], when closely compared with similar CGO and MLO data, should directly reflect the impact of rising Asian emissions on global CO_2 levels. With regard to future monitoring strategies, as the ^{14}C bomb pulse is decaying to levels that make the impact of fossil-fuel changes more detectable, access to precision ^{14}C measurements[29] offers a direct way to resolve the ambiguity between fossil and modern terrestrial carbon fluxes in the Northern Hemisphere.

Methods

The CSIRO CO_2 data that underpin this paper are unusual in some important aspects that are described in detail elsewhere[5] and summarized briefly here. Over the two recent decades of interest, CO_2 measurements by both gas chromatograph (global, flask sampling) and the ultraprecise infra-red LoFlo analyser (CGO, continuous) are characterized by unusually low gas consumption[19,20,30] with each instrument independently calibrated relative to the World Meteorological Organization CO_2 Mole Fraction Scale. The low consumption translates into greatly simplified and extensively verified reference gas characterization (that is, high and robust temporal precision); in particular, the Cape Grim LoFlo has maintained temporal precision at better than 10 ppb in routine monthly calibrations against seven dedicated World Meteorological Organization-calibrated high-pressure cylinder standards since 2003.

Sampling strategies to avoid regional influence are used at all CSIRO sites, most stringently at Cape Grim, and most comprehensively using the continuous LoFlo analyser; this samples around 200 h each month that have at least 10-day back trajectories over the Southern Ocean, confirmed by radon measurements[31]. The LoFlo data support the integrity of CGO flask sampling criteria. Scatter in monthly average data at all sites is interpreted as a proxy for spatial representativeness. The selection of MLO and CGO as main sites to define the inter-hemispheric gradient is underpinned by the small vertical gradients obtained from intensive vertical profiling at each site[32].

Unlike a previous attempt[5], CO_2 variability resulting from wildfires is specifically addressed using monthly global CO_2 emissions from the Global Fire Emissions Database[16] (GFED3). Similarly, monthly concentrations are corrected for CO_2 reduction accompanying major volcanic eruptions[33] involving climate-induced terrestrial and oceanic exchanges extending beyond the aerosol pertubation[17] (Supplementary Fig. S6). The overall IAV contribution to decadal dC/dt variability turns out to be relatively small and only marginally changed by the upgraded approach.

A pair of inversions (differing only in the choice of assumed fossil emissions) was run with each of two different inversion systems, CCAM (ref. 18) and Jena[23], to estimate land and ocean carbon fluxes. The two inversion systems differ by their flux estimation methods, the spatial resolution of fluxes solved for (146 regions for CCAM, 5° × 3.75° grid cell for Jena), the choice of atmospheric CO_2 data and its application in the inversion, whether inter-annually varying transport was incorporated or not, and their choices of prior flux information. The CCAM inversion system was run from 1992–2008 and used a fixed spatial distribution[3] for fossil emissions; with either the temporal variation of the reported fossil emissions or increasing linearly interpolated annual emissions (from 6.03 Pg C yr^{-1} in 1990 to 8.44 Pg C yr^{-1} in 2008). The Jena inversion system was run from 1994–2010 with fossil emissions taken from EDGAR 4.0 or linearly increasing (from 6.64 Pg C yr^{-1}

in 1994 to 9.49 Pg C yr^{-1} in 2010). Fluxes estimated by the inversions were analysed for 90°–20° S, 20° S–20° N and 20°–90° N and separately for land and ocean. To determine the quality of the data fit, $RMSD = \sqrt{(\sum(c_{INV} - c_{OBS})^2/N)}$ is summed across all sites and measurement times, where c_{INV} is the estimated atmospheric concentrations from the inversion and c_{OBS} is the observations.

The contribution of fossil emissions to atmospheric CO_2 concentrations at Cape Grim and Mauna Loa was modelled using CCAM nudged with NCEP winds for 1988–2011. Two tracers were simulated. Both used a fixed spatial distribution of fossil emissions[3], with emissions growing in time either linearly or as reported previously[3,9]. From 2010, another simulation varied the spatial resolution so that emission increases occurred from 70°–150° E, 15°–40° N (Asian region). To represent CGO, the model output was sampled at the grid point to the southwest of the location of Cape Grim (to approximate baseline selection) in the lowest model level. For MLO, we used the nearest grid point horizontally and model level 7 (approximately 2.9 km).

Received 26 July 2012; accepted 7 January 2013; published online 10 February 2013

References

1. Trudinger, C. M., Enting, I. G., Etheridge, D. M., Francey, R. J. & Rayner, P. J. in *A History of Atmospheric CO_2 and Its Effect of Plants, Animals and Ecosystems* (eds Ehleringer, J. R., Cerling, T. E. & Dearing, M. D.) 329–349 (Ecological Studies, Vol. 177, Springer, 2005).
2. Keeling, C. D. *et al.* in *A History of Atmospheric CO_2 and Its Effects on Plants, Animals, and Ecosystems* (eds Ehleringer, J. R., Cerling, T. E. & Dearing, M. D.) 83–113 (Ecological Studies, Vol. 177, Springer, 2005).
3. Boden, T. A., Marland, G. & Andres, R. J. *Global, Regional, and National Fossil-fuel CO_2 Emissions* (Carbon Dioxide Information Analysis Center, 2010) http://cdiac.ornl.gov/trends/emis/overview.html.
4. Houghton, R. A. in *TRENDS: A Compendium of Data on Global Change* (Carbon Dioxide Information Analysis Center, 2008); available at http://cdiac.esd.ornl.gov/trends/landuse/houghton/houghton.html.
5. Francey, R. J. *et al.* Differences between trends in atmospheric CO_2 and reported trends in anthropogenic CO_2 emissions. *Tellus* **62,** 316–328 (2010).
6. Le Quéré, C., Raupach, M. R., Canadell, J. G. & Marland, G. Trends in the sources and sinks of carbon dioxide. *Nature Geosci.* **2,** 831–837 (2009).
7. Peters, G. P. *et al.* Rapid growth in CO_2 emissions after the 2008–2009 global financial crisis. *Nature Clim. Change* **2,** 2–4 (2012).
8. Friedlingstein, P. *et al.* Update on CO_2 emissions. *Nature Geosci.* **3,** 811–812 (2010).
9. Andres, R. J. *et al.* Synthesis of carbon dioxide emissions from fossil-fuel combustion. *Biogeosciences* **9,** 1845–1871 (2012).
10. Guan, D., Liu, Z., Geng, Y., Lindner, S. & Hubacek, K. The gigatonne gap in China's carbon dioxide inventories. *Nature Clim. Change* **2,** 672–675 (2012).
11. Marland, G. Emissions accounting: China's uncertain CO_2 emissions. *Nature Clim. Change* **2,** 645–646 (2012).
12. Ballantyne, A. P., Alden, C. B., Miller, J. B., Tans, P. P. & White, J. W. C. Increase in observed net carbon dioxide uptake by land and oceans during the past 50 years. *Nature* **488,** 70–72 (2012).
13. Pan, Y. *et al.* A large and persistent carbon sink in the world's forests. *Science* **333,** 988–993 (2011).
14. Sarmiento, J. L. *et al.* Trends and regional distributions of land and ocean carbon sinks. *Biogeosciences* **7,** 2351–2367 (2010).
15. Le Quéré, C., Takahashi, T., Buitenhuis, E. T., Rödenbeck, C. & Sutherland, S. C. Impact of climate change and variability on the global oceanic sink of CO_2. *Glob. Biogeochem. Cycles* **24,** GB4007 (2010).
16. Van der Werf, G. *et al.* Global fire emissions and the contribution of deforestation, savanna, forest, agricultural, and peat fires (1997–2009). *Atmos. Chem. Phys.* **10,** 11707–12010 (2010).
17. Frölicher, T. L., Joos, F. & Raible, C. C. Sensitivity of atmospheric CO_2 and climate to explosive volcanic eruptions. *Biogeosciences* **8,** 2317–2339 (2011).
18. Rayner, P. J. *et al.* The interannual variability of the global carbon cycle (1992-2005) inferred by inversion of atmospheric CO_2 and $^{13}CO_2$ measurements. *Glob. Biogeochem. Cycles* **22,** GB3508 (2008).
19. Francey, R. J. & Steele, L. P. Measuring atmospheric carbon dioxide—The calibration challenge. *Accredit. Qual. Assur.* **8,** 200–204 (2003).
20. Francey, R. J. *et al.* in *Baseline Atmospheric Program (Australia) 1993* (eds Francey, R. J., Dick, A. L. & Derek, N.) 8–29 (Bureau of Meteorology and CSIRO Division of Atmospheric Research, 1996).
21. Yevich, R. & Logan, J. A. An assessment of biofuel use and burning of agricultural waste in the developing world. *Glob. Biogeochem. Cycles* **17,** 1095 (2003).
22. Knorr, W. Is the airborne fraction of anthropogenic CO_2 emissions increasing? *Geophys. Res. Lett.* **36,** L21710 (2009).
23. Rödenbeck, C., Houweling, S., Gloor, M. & Heimann, M. CO_2 flux history 1982–2001 inferred from atmospheric data using a global inversion of atmospheric transport. *Atmos. Chem. Phys.* **3,** 1919–1964 (2003).
24. http://www.esrl.noaa.gov/psd/data/gridded/data.ncep.reanalysis.html.
25. Dargaville, R. J., Law, R. M. & Pribac, F. Implications of interannual variability in atmospheric circulation on modeled CO_2 concentrations and source estimates. *Glob. Biogeochem. Cycles* **14,** 931–943 (2000).
26. Le Quéré, C. *et al.* Saturation of the Southern Ocean CO_2 sink due to recent climate change. *Science* **316,** 1735–1738 (2007).
27. Manning, M. *et al.* Misrepresentation of the IPCC CO_2 emission scenarios. *Nature Geosci.* **3,** 376–377 (2010).
28. http://www.wmo.int/pages/prog/arep/gaw/gaw_home_en.html.
29. Levin, I. *et al.* Observations and modelling of the global distribution and long-term trend of atmospheric $^{14}CO_2$. *Tellus* **62B,** 26–46 (2010).
30. Steele, L. P. *et al.* in *Baseline Atmospheric Program (Australia) 1999–2000* (eds Tindale, N. W., Derek, N. & Fraser, P. J.) 80–84 (Bureau of Meteorology and CSIRO Atmospheric Research, 2003).
31. Zahorowski, W. *et al.* Radon-222 in boundary layer and free tropospheric continental outflow events at three ACE-Asia sites. *Tellus B* **57,** 124–140 (2005).
32. Stephens, B. B. *et al.* The vertical distribution of atmospheric CO_2 defines the latitudinal partitioning of global carbon fluxes. *Science* **316,** 1732–1735 (2007).
33. Jones, C. D. & Cox, P. M. Modeling the volcanic signal in the atmospheric CO_2 record. *Glob. Biogeochem. Cycles* **15,** 453–465 (2001).
34. *Statistical Review of World Energy* (BP, 2011); available via http://go.nature.com/jrUwIm.
35. European Commission. Emissions Database for Global Atmospheric Research (EDGAR). Europa—EDGAR Overview http://edgar.jrc.ec.europa.eu/overview.php?v540 (2009).
36. Thoning, K. *et al.* Atmospheric carbon dioxide at Mauna Loa observatory, 2, Analysis of the NOAA/GMCC data, 1974–1985. *J. Geophys. Res.* **94,** 8549–8565 (1989).
37. Enting, I. G. *et al.* Propagating data uncertainty through smoothing spline fits. *Tellus B* **58,** 305–309 (2006).
38. Conway, T. J., Lang, P. M. & Masarie, K. A. Atmospheric carbon dioxide dry air mole fractions from the NOAA ESRL carbon cycle cooperative global air sampling network, 1968–2010, Version: 2011-10-14 (2011); available at ftp://ftp.cmdl.noaa.gov/ccg/co2/flask/event/.

Acknowledgements

G. Pearman's emphasis on global representativeness during establishment of Australian CO_2 monitoring underpins this work. Data used in this report are routinely submitted to the World Data Centre for Greenhouse Gases and CDIAC international databases (but in formats that preclude the data selection and uncertainty propagation used in this paper). More comprehensive and recent data, including LoFlo data, are available to researchers by contacting paul.krummel@csiro.au. CSIRO GASLAB staff and the Australian Bureau of Meteorology/Cape Grim Baseline Air Pollution Station continue to provide excellence in the operation of developmental equipment and in collection and processing of samples and data. Collection of samples at other sites is carried out with assistance from NOAA (USA), Environment Canada, Australian Antarctic Division and Australian Bureau of Meteorology. R.J.F, M.v.d.S., P.B.K., R.L.L., L.P.S and C.E.A. have been partly financially supported by the Bureau of Meteorology through the Cape Grim programme. R.J.A. was sponsored by US Department of Energy, Office of Science, Biological and Environmental Research (BER) programmes performed at Oak Ridge National Laboratory (ORNL) under US Department of Energy contract DE-AC05-00OR22725. CSIRO co-authors have been partly financially supported by the ACCSP (Australian Climate Change Science Program) through the Department of Climate Change and Energy Efficiency. A.R.S. is partially supported by an OCE (Office of Chief Executive) post-doctoral award. CCAM model simulations were undertaken on the NCI National Facility in Canberra, Australia, which is supported by the Australian Commonwealth Government. Valuable comments have been received from Y-P. Wang, P. Canadell, P. Rayner and A. Lenton.

Author contributions

R.J.F, C.M.T. and R.M.L took lead roles in writing this paper. M.v.d.S., R.L.L, L.P.S and C.E.A. contributed to the design and quality control of measurements and P.B.K. developed and provided data processing. R.J.A. provided anthropogenic emissions data and advice. R.M.L. and C.R. designed, and with A.R.S., carried out inversion modelling tests. All authors advised on the manuscript.

Additional information

Supplementary information is available in the online version of the paper. Reprints and permissions information is available online at www.nature.com/reprints. Correspondence and requests for materials should be addressed to R.J.F.

Competing financial interests

The authors declare no competing financial interests.